$^{11}B\{^{15}N\}$ REDOR AND ^{11}B SPIN ECHO STUDIES FOR STRUCTURAL CHARACTERIZATION OF Si-B-C-N PRECURSOR CERAMICS

Otgontuul Tsetsgee, Institute of physics and technology, MAS, Mongolia
Klaus Mueller, A Institut fuer Physikalische Chemie, Universitaet Stuttgart, Germany

Abstract

A Solid-state NMR spectroscopy is employed for the structural characterization of precursorderived Si-B-C-N ceramics. Particular emphasis is given to the structural composition of the BNCx phase which plays a key role for the unusual high temperature stability of these materials. In the present work $^{11}B(^{15}N)$ REDOR and ^{11}B spin echo experiments are presented for two ^{15}N enriched precursor systems, made from substituted polysilazanes and polysilylcarbodiimides, which provide interatomic boron-boron and boron-nitrogen distances. The obtained results are compatible with the presence of layered structures as reported for hexagonal boron nitride [h-B]. The derived boron-nitrogen and boron-boron distances, however, are larger than in h-BN, reflecting some layer distortions. The boron-boron distances are found to decrease with increasing pyrolysis temperature, whereas the boron-nitrogen distances remain practically unaltered at elevated pyrolysis temperatures. On the basis of the present results it is concluded that intercalated BN.and sp^2-carbon layers most likely constitute the BNC_x phase. The graphite-like carbon layers are assumed to create some internal pressure, which in turn is responsible for the observed interatomic distance increase in the BN layers. However, other scenarios, like the direct incorporation of small sp^2-carbon domains into the BN-sheets, cannot be ruled out completely. Further work along this line appears to be necessary to develop a comprehensive structural model for the BNC_x phase in such quarternary ceramic systems.

Keywords: Solid-state NMR, Si-B-C-N ceramic, Precursor ceramic
Soft materils.4(2-4),207-225

INTRODUCTION

Silicon nitride- and silicon nitride/silicon carbide-based composites exhibit exceptional material properties for instance creep and corrosion resistance, high tensile strength and hardness and therefore possess a great potential for high-temperature applications. In the past, such ceramics were prepared by sintering of silicon nitride and silicon carbide powders. The sintering additives [1, 2] required for the ceramic preparation, however, put an upper limit for the high-temperature applicability of these materials [3]. More recently, another preparation route without sintering aids was introduced, which is based on the pyrolysis of suitable pre-ceramic [polymeric] precursors [4–8]. In general, the ceramic samples obtained via this precursor route exhibit a much better homogeneity on the molecular level. Moreover, the latter precursor route offers a better flexibility for the design of ceramic tools.

During recent years, the precursor route, i.e., from the precursor polymer to the final crystalline ceramics, has been studied in great detail employing a great variety of experimental techniques [9]. It was demonstrated that the polymer-to-ceramic conversion comprises various amorphous intermediates, until the amorphous ceramic is formed at about 1000°C. Upon further heating crystallization sets in, giving rise to thermodynamically stable phases beyond about 1300°C [7]. Previous studies have shown that the specific bulk properties of ternary Si-C-N ceramics strongly depend on the molecular composition and the [local] molecular structure, both of which can be altered by the choice of the corresponding precursor polymers.

More recently, it has been demonstrated that quarternary Si-B-C-N ceramics, derived from suitable boron-modified polymers, possess a temperature stability that is superior to the aforementioned Si-C-N ceramics [7, 10–12]. The majority of studies on such ceramic systems used polysilazanes and polysilylcarbodiimides as precursor polymers, which upon hydroboration and subsequent heat-treatment yielded amorphous or crystalline quaternary ceramics [13]. It is anticipated that the thermal stability of Si-B-C-N ceramics primarily relies on their unique structural composition, consisting of nanocrystalline SiC and Si_3N_4 domains as well as a turbostratic BNC_x phase [14–16].

As mentioned earlier, the polymer-to-ceramic conversion also involves several amorphous intermediate steps which rules out common

techniques, such as X-ray diffraction, for structural characterization. In this connection, solid-state NMR spectroscopy has demonstrated its particular potential to unravel the structural features of all intermediate steps, also including the amorphous species [17–20]. NMR spectroscopy probes the molecular environment (short-range order up to a few Å) around selected nuclei, whose magnetic properties strongly depend on the local electronic environment and dipolar interactions with nuclei in the next neighborhood. Furthermore, NMR spectroscopy is of particular attraction for ternary and quaternary oxide-free ceramics, as they possess several NMR-active nuclei—^{13}C, ^{29}Si, ^{1}H or ^{11}B—which can be studied directly without further isotopic enrichment [21–34].

In the present contribution, solid-state NMR spectroscopy is employed to monitor the structural changes during the pyrolysis of two representative boron-modified polyvinylsilazane and polyvinylsilylcarbodiimide precursors [see Fig. 1] and the formation of amorphous and crystalline Si-B-C-N ceramics. Particular emphasis is given to the structural evolution of the aforementioned BNC_x phase which was evidenced by TEM and other techniques [14–16], andwhich plays an important role for the high temperature stability of these quaternary ceramics. However, a satisfactory and complete picture about the structural composition of the BNC_x phase is still missing. Hence, it is open whether well separated boron nitride and graphite-like domains exist, whether separated but intercalated layers are formed or whether a homogenous distribution of nanosized BN and graphite-like domains (interdigitated structure) has to be discussed.

The work reported here relies on 11B NMR studies, comprising for the first time ^{11}Bf ^{15}Ng REDOR (rotational echo double resonance) [35–40] and ^{11}B spin echo experiments [39, 41–43] on ^{15}N enriched samples, from which (heteronuclear) boron-nitrogen and (homonuclear) boron-boron internuclear distances are obtained. The REDOR experiment is a spin echo experiment under MAS conditions where in the present case the heteronuclear dipolar interaction between the ^{11}B and ^{15}Nnuclei is recoupled through irradiation at the ^{15}N frequency (.e., p pulses at multiples of ½ rotor period). The REDOR signal is obtained from difference measurements with and without ^{15}N irradiation. It can be analyzed in a quantitative way, and provides internuclear boron-nitrogen distances. Likewise, the signal decay in a standard ^{11}B spin echo experiment, performed with static samples, is used to derive via the second moment internuclear boron-boron distances in the present ceramic materials. It is shown that such experimental NMR techniques, which exploit hetero- and homonuclear dipolar interactions and which successfully have been applied for instance in glasses [39], are well suited for the structural characterization of precursor-derived ceramics. The derived internuclear distances are somewhat

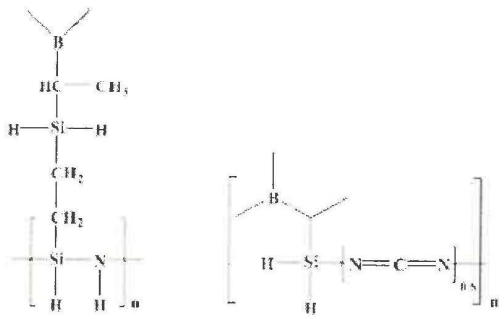

1 2

Figure 1. Chemical structures of the precursor 1 and 2

larger than in pure hexagonal boron nitride. Moreover, they are found to depend on the actual pyrolysis stage of the polymer-to-ceramic transformation and to some extent also on the composition of the precursor polymer.

EXPERIMENTAL

Synthesis. 99 atom % ^{15}N enriched ammonia was used for the synthesis of both precursor polymers. Precursor polymer-1, boron modified polyvinylsilizane, was obtained by reaction of oligovinylsilazane $([H_2C{=}CH]SiHNH)n$ with tris[hydrosilylethyl]boranes $B\{C_2H_4SiH_3\}_3$. Here, the ^{15}N enriched ammonia was used during the preparation step of the oligovinylsilazane which yielded 99 atom % ^{15}N enriched precursor polymer-1. Further details about the synthetic procedures can be found elsewhere [44]. Boron modified polysilylcarbodiimide (precursor polymer-2, $(B[C_2H_4\text{-}SiH_2\text{-}(NCN)_{0.5}]_3)_n$ was synthesized from tris(hydridosilylethyl)- borane $(B[C_2H_4\text{-}SiH_3]_3)_n$ and 50 atom % ^{15}N enriched cyanamide [borane-cyanamide ratio = 1:1.5], as described in Refs. [45] and [46]. The enriched cyanamide was obtained by reaction of 99 atom % ^{15}N enriched ammonia with bromocyan. All chemical reactions were performed in argon atmosphere.

Thermolysis. Samples were prepared by pyrolysis of 1 to 2 g of the polymeric precursor in a quartz or aluminium oxide tube under a steady flow (50

ml/min) of purified argon in a programmable tube furnace (Gero HTRV 40-250). Starting at ambient temperature, the following heating program was used: (i) an initial 1 K/min ramp to the desired thermolysis temperature, (ii) a 2 h hold at the thermolysis temperature [samples heat treated at 1400°C], and (iii) sample cooling with a rate of 2 K/min, during which the sample was allowed to cool to room temperature. Annealing at higher temperatures [1600–2000°C] was done on samples thermolyzed at 1400°C/2 h in argon atmosphere. The heating and cooling rates were 20 K/min to 1400°C, 2°C to the desired annealing temperature [dwell time: 5 h] and 20 K/min to room temperature.

NMR measurements. All solid-state NMR experiments were carried out on a Varian InfinityPlus 400 spectrometer operating at a static magnetic field of 9.4 T using a 4 mm triple resonance HXY probe. The resonance frequencies were 40.5, 79.41 and 128.26 MHz, for ^{15}N, ^{29}Si and ^{11}B, respectively. ^{29}Si chemical shifts were determined relative to the external standard Q_8M_8 [the trimethylsilylester of octametric silicate] which were then recalculated relative to TMS (δ = 0 ppm). ^{11}B NMR spectra are referenced against $BF_3 . OEt_2$ [δ = 0 ppm].

^{29}Si NMR spectra were recorded under MAS condition [sample rotation frequency: 5 kHz] by direct excitation applying p/4 pulses of 2.3 ms in width, and recycle delays of 45 s. $^{11}B\{^{15}N\}$REDOR experiments (see Fig. 2) were done at a sample spinning frequency of 10 kHz and recycle delays between 2 and 15 s depending on the ^{11}B spin-lattice relaxation time. ^{11}B p/2 and p pulse widths were 1 and 1.95 ms, respectively, while the ^{15}N dephasing p pulse width was 7 ms. The various pulse lengths and amplitudes were optimized directly on the sample in order to achieve maximum signal intensity and dephasing effects. ^{11}B spin-echo experiments were done (see Fig. 2) under static conditions with the same pulse widths and recycle delays as for the REDOR experiments. During the ^{11}B NMR the number of scans varied between 64 and 256 depending on the actual signal-to-noise ratio of the samples.

Data analysis. Numerical simulations were done with laboratory written MATLAB routines and the SIMPSON program package [47], employing the direct method in conjunction with the REPULSION set of 100 angles [48], to test whether the ^{11}B-^{11}B dipolar couplings influence the $^{11}B\{^{15}N\}$ REDOR signals. They showed that the effect of the homonuclear couplings on the dephasing of the ^{11}B-nucleus is negligible in our experiments. The final fitting of the REDOR curves was therefore done with a laboratory written MATLAB routine, which uses purely heteronuclear ^{11}B-^{15}N couplings, based on the equations described in Ref. [49].

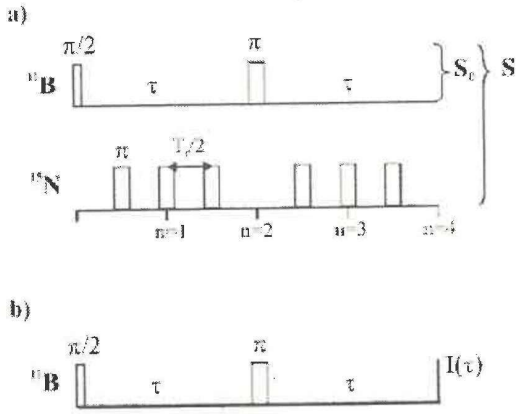

Figure 2. *^{11}B-^{15}N REDOR (a) and ^{11}B spin echo pulse (b) sequences employed in the present work (TR: rotor period, n: number of rotor periods).*

The program variables are the number of coupled spins, the bond orientations and bond lengths. In addition, a scaling factor was introduced which accounts for the fact that the experimental REDOR curves do not reach the full attenuation level DS/S0 = 1.0. Representative model calculations have shown that the MATLAB routines and the SIMPSON program provide identical results.

For the final $^{11}B\{^{15}N\}$REDOR simulations of the samples from precursor polymer 1, with 99 atom % ^{15}N enrichment, only the first coordination sphere was considered with three ^{15}N nuclei and identical distance from the central ^{11}B nucleus, i.e., a IS3 spin system (I = ^{11}B, S = ^{15}N) with an S-I-S bond angle of 120°. Due to the aforementioned synthetic reasons, only 50 atom % ^{15}N enrichment could be achieved for precursor polymer 2 and the derived ceramics. Hence, the theoretical REDOR curves represent a summation of the curves from IS_3, IS_2, IS and I spin systems with statistical weights of 1/8, 3/8, 3/8 and 1/8, respectively, and the ideal S-I-S angle of 120°. The estimated error for the given boron-boron distances is +2%.

The analysis of the ^{11}B spin echo decay curves of the static samples is based on analytical

expressions, as given in Ref. [41–43]. The spin echo intensity I(2t) thus depends on the second moment M_2 by

$$I(2\tau) = I(0)\exp\left\{-\frac{1}{T_2}(2\tau)^2\right\} = I(0)\exp\left\{-\frac{M_2}{2}(2\tau)^2\right\} \qquad (1)$$

By application of the van Vleck equations, the second moments for homoor heteronuclear dipolar coupled systems provide distance information [14]. For the case of homonuclear coupled spin-3/2 nuclei, the second moment [for a powder average of the sample] is given by

$$M_2 = 0.9562\left(\frac{\mu_0}{4\pi}\right)^2 \gamma^4 \hbar^2 \sum_j \left(\frac{1}{r_{ij}}\right)^6 \qquad (2)$$

where the summation runs over all coupled nuclei j at distances r_{ij}. Accordingly, the experimental second moment data from the present ^{11}B spin echo decays were inserted in equation (2) to derive the average boronboron distances ,r. in the various ceramic samples. Here, only the six closest boron nuclei with identical distances from the central ^{11}B nucleus were considered. The summation over only six boron nuclei in equation (2) then yields 4.86/,r.6 where the pre-factor accounts for the natural abundance of the ^{11}B nuclei. The estimated error for the given boronboron distances is +3%.

RESULTS AND DISCUSSION

In the following, we report on solid-state NMR studies of the pyrolysis of boron-modified polyvinylsilzane-1 and polyvinylsilylcarbodiimide-2, from which quaternary Si-B-C-N ceramics are formed. Former studies have demonstrated that this precursor route provides ceramic materials of very homogeneous elemental composition and unusual thermal stability [7, 10–12]. The polymer-to-ceramic conversion has been studied extensively by a variety of experimental techniques [14–20]. It was shown that during the earlier stages of the pyrolysis, a cross-linking of the polymer occurs, followed by the formation of a pre-ceramic network above 600°C. The transformation to the amorphous ceramic is completed at about 1050°C, which is characterized by a "Si-C-N" matrix, amorphous sp^2-carbon and "B-C-N" domains (or BNC_x phase). Above 1300°C crystallization sets in, along with the formation of nanocrystalline SiC and Si_3N_4 domains as well as a turbostratic BNC_x phase. In the present work, we primarily address the structural features of the boron-containing ceramic components which are examined by $^{11}B\{^{15}N\}$ REDOR and ^{11}B spinecho experiments.

. To emphasize the differences for the two precursor systems, representative ^{29}Si NMR spectra are shown in Figs. 3 and 4 for the samples after pyrolysis to 1050°C and 1400°C, referring to the amorphous ceramic and the onset of crystallization. The broad ^{29}Si NMR spectra reflect a superposition of ^{29}Si resonances arising from silicon nuclei with different coordination spheres, i.e., structural units with the formal composition SiC_xN_{4-x} with x = 1 to 4. The ^{29}Si NMR spectra are therefore characteristic for the presence of a "S-C-N" matrix where the silicon atoms are coordinated by nitrogen and carbon atoms of different relative amount.

In the ^{29}Si NMR spectra of precursor polymer-2 (see Fig. 4) the highfield spectral component around -44 ppm is clearly evident which reflects the presence of SiN_4 units (i.e., silicon nitride domains) and which is of

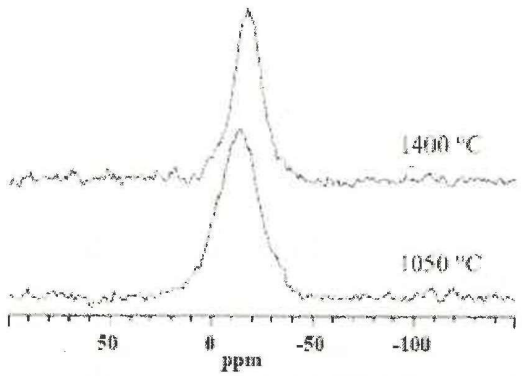

Figure 3. *Representative ^{29}Si NMR spectra of the Si-B-C-N ceramic samples obtained for precursor polymer-1 after pyrolysis with a maximum temperature given in the figure.*

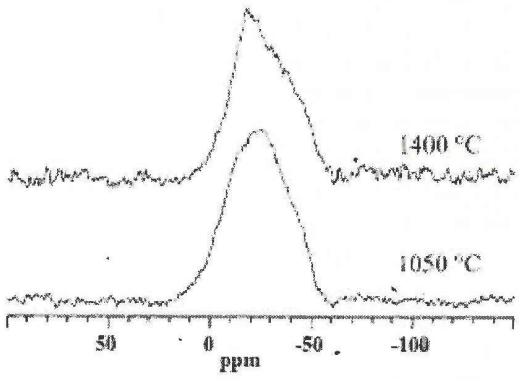

Figure 4. *Representative ^{29}Si NMR spectra of the Si-B-C-N ceramic samples obtained for precursor polymer-2 after pyrolysis with a maximum temperature given in the figure.*

much weaker intensity in the spectra of polymer-1. This result can be understood by the higher nitrogen content in the polymeric precursor-2, and is in agreement with former ^{29}Si NMR studies on related precursor systems starting from silazanes or silylcarbodiimides [21–34]. It reflects the competition between boron and silicon to coordinate nitrogen and the higher affinity of boron to bind nitrogen. The relative amount of nitrogen (with respect to silicon) in the carbodiimide precursor-2 is higher (Si:N ratio = 1:1) than for silazane-1 (Si:N ratio = 2:1), and the B:N ratio is the same for both precursor systems. After formation of the boron nitride domains, more nitrogen can be bound to silicon in system-2, in agreement with the higher amount of SiN_4 units for this precursor system. Hence, for system-2 a larger structural heterogeneity is expected in the Si-C-N domains, as also demonstrated experimentally by the broader ^{29}Si NMR spectra covering the whole spectral range for the various SiC_xN_{4-x} components. For precursor system-1 with a smaller overall ^{29}Si NMR spectral width the structural heterogeneity is reduced. Here, due to the lower nitrogen content the structural components with higher nitrogen content–given by the high–field signal components— are less probable.

Former ^{13}C NMR investigations on such precursor systems have shown that above 800 °C domains with amorphous sp^2-carbon are formed, which are assumed to exhibit a graphite-like structure and whose relative amount depends on the chemical composition of the precursor polymer (i.e., carbon content) [21–34].

Figure 5 shows a representative series of ^{11}B NMR spectra for precursor system-2 recorded under MAS conditions covering the whole temperature range from 400°C to 1900°C. In general, broad ^{11}B resonances are observed which become somewhat narrower above 800°C at which the amorphous ceramic is formed. Upon further heating, they remain almost unaltered apart from some additional broadening above 1700°C. The ^{11}B NMR spectra of the amorphous ceramic at 1050°C and above exhibit a second order quadrupolar broadening for boron nuclei that are trigonally coordinated by nitrogen atoms (see Fig. 6). At the present magnetic field strength of 9.4 T this quadrupolar broadening is much less pronounced than at lower fields (B ≤ 7 T) used during earlier studies, where central transition ^{11}B NMR line shapes were observed with a characteristic second order broadening. From the respective line shape simulations and from SATRAS experiments [12, 26, 50] a quadrupolar coupling constant of 2.9 MHz was derived, which is identical to the value reported for pure hexagonal boron nitride (*h*-BN). In this context, it is worthwhile to note that so far there is no proof for the formation of direct boron-carbon bonds. Even the observed chemical shift values are only compatible with the presence of boron-nitrogen bonds. Hence, it was concluded that the amorphous ceramics consist of a "Si-C-N" matrix with silicon atoms in mixed coordination, which are separated from domains of amorphous sp^2-carbon and regions with h-BN.

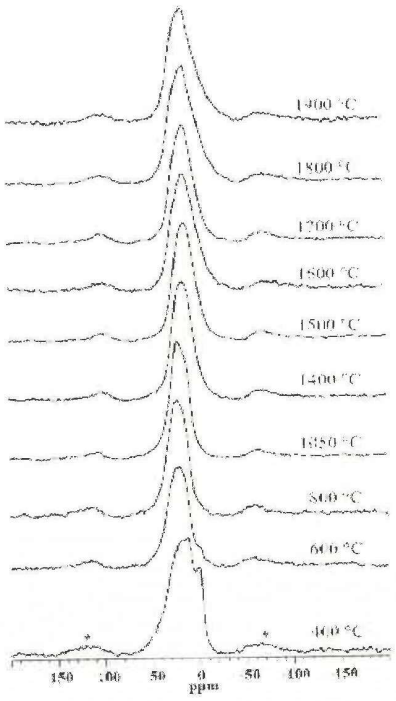

FIGURE 5 *11B NMR spectra of the Si-B-C-N ceramic samples obtained for precursor polymer-2 after pyrolysis with the maximum temperature given in the figure. Asterisks indicate spinning sidebands.*

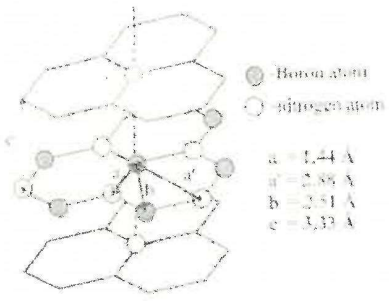

Figure 6 *Schematic drawing of the hexagonal boron nitride sheets expected in the present Si-B-CN ceramic samples (a, a0, b: in-plane distances, c: inter-plane distance).*

At the same time, TEM results gave evidence for the presence of a turbostratic BNC_x phase (containing only boron, carbon, and nitrogen) in the amorphous ceramic stage and beyond [14–16] which is assumed to play a key role for the high-temperature stability of Si-B-C-N ceramics. However, so far further details about the structural composition of the BNC_x are missing. We therefore underwent a solid-state NMR study which should shed further light on the structural composition of the BNC_x domains. Hence, $^{11}B\{^{15}N\}$ REDOR and ^{11}B spin echo experiments (see Fig. 2) were performed which provide for the first time (heteronuclear) boronnitrogen and (homonuclear) boron-boron distances in such quaternary ceramics. It should be mentioned that similar double resonance NMR experiments were performed earlier on another Si-B-C-N ceramic system, for which only one ^{13}C and ^{15}N enriched sample, heat-treated at one particular temperature, was available [51]. Among other experiments, $^{15}N\{^{11}B\}$ REAPDOR (rotational-echo adiabatic-passage doubleresonance) spectra were reported which also provide boron-nitrogen distance information. However, the spectral resolution was too low, and a quantitative data analysis was therefore not possible. $^{11}B\{^{15}N\}$REDOR or ^{11}B spin echo experiments were not performed during that earlier work. The particular advantage of our present study is that a series of samples, pretreated at different temperatures, is available which also allows a systematic study of the whole pyrolysis process.

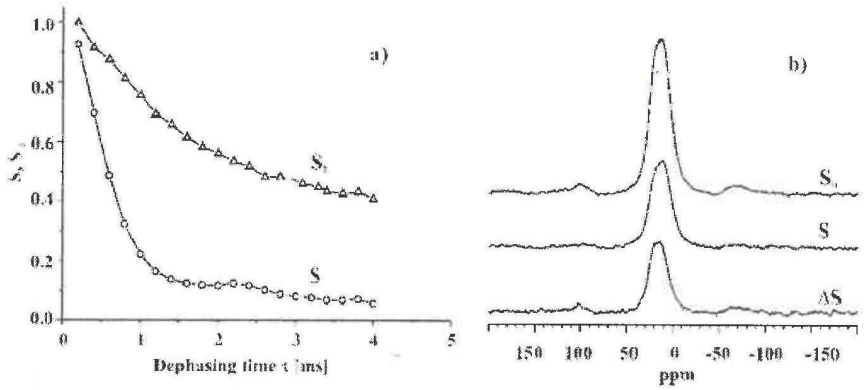

Figure 7. a) Experimental REDOR decay curves with (S) and without (S0) ^{15}N irradiation. B) Experimental 11Bf15Ng REDOR spectra without (top) and with (bottom) 15N irradiation obtained after 6 rotor cycles. The signals were recorded for a sample from precursor polymer-2 after pyrolysis with a maximum temperature of 1400˚C.

Figure 7 shows two representative echo decay curves for sampled from precursor system-2 heated to 1400 ° C, obtained from the present $^{11}B\{^{15}N\}$REDOR experiments with (S) and without (S0) the presence of the ^{15}N π pulses, along with two $^{11}B\{^{15}N\}$ REDOR spectra obtained from the Fourier transformed echo signal after 6 rotor periods. Here, due to the additional dephasing from the ^{11}B-^{15}N dipolar interactions the signal S decays considerably faster than the reference signal S_0 whose decay is only determined by a residual T_2 contribution. From such decay curves then the corresponding REDOR curves are calculated.

Representative experimental $^{11}B\{^{15}N\}$REDOR curves for both precursor systems are depicted in Figs. 8 and 9 along with their theoretical counterparts. In general, the given examples Representative experimental $^{11}B\{^{15}N\}$ REDOR curves for both precursor systems are depicted in Fig.8 and 9 along with their theoretical counterparts. In general, the given examples display a good and satisfactory agreement between experiment and theory. The most important part of the REDOR curves is the initial slope which is dominated by the shortest boron-nitrogen distance, and which can be related to the second moment accounting for heteronuclear ^{11}B-^{15}N dipolar interactions [39]. The plateau value of the REDOR curve indicates the percentage of boron atoms that are bound to nitrogen. As outlined in the experimental part, the simulations for system-1 with 99 atom % ^{15}N enrichment were done by assuming a planar IS_3 spin system (I = ^{11}B, S = ^{15}N) with identical bond lengths and ideal S-I-S bond angles of 120°. For system-2 with only 50 atom % ^{15}N enrichment the given theoretical REDOR curves are superpositions of the corresponding weighted curves for IS3, IS2 , IS and I spin systems, again assuming identical bond lengths and

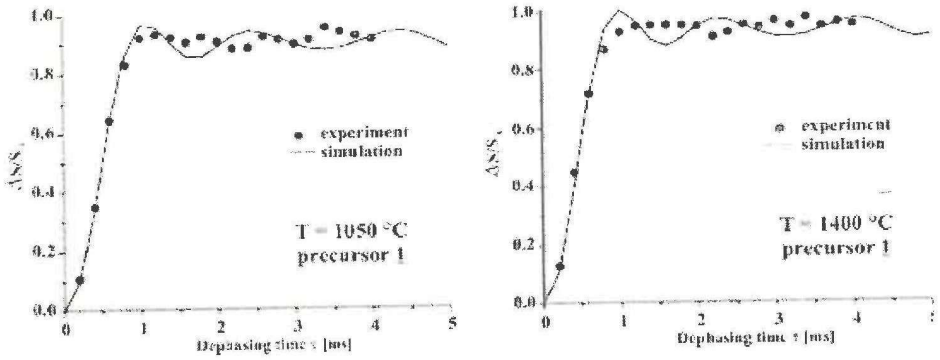

FIGURE 8. *Experimental 11B-15N REDOR curves obtained for Si-B-C-N ceramic samples from precursor polymer 1 after yrolysis with a maximum temperature given in the figure. The theoretical curves were obtained with the parameters given in Table 1 and the model discussed in the experimental section.*

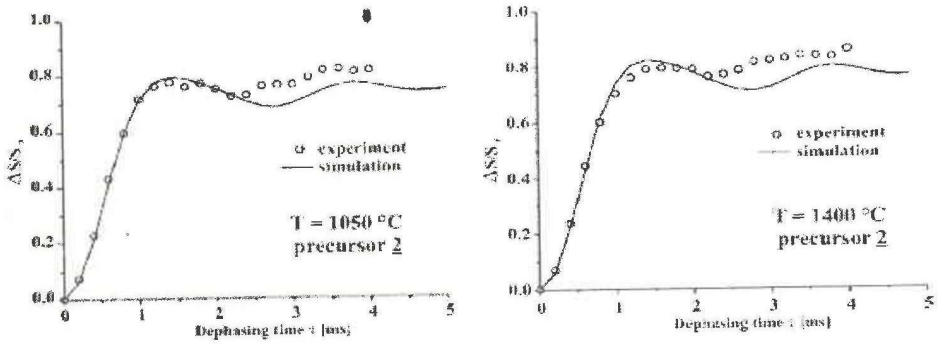

FIGURE 9. *Experimental 11B-15N REDOR curves obtained for Si-B-C-N ceramic samples from precursor polymer-2 after pyrolysis with a maximum temperature given in the figure. The theoretical curves were obtained with the parameters given in Table 1 and the model discussed in the experimental section.*

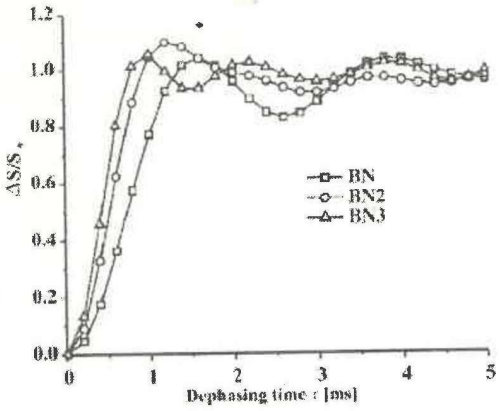

FIGURE 10. *Theoretical 11B-15N REDOR curves obtained by considering a boron nucleus coordinated by three (BN3), two (BN2) and one (BN) nitrogen nuclei at a distance of 1.58Å and N-B-N angles of 120°.*

ideal bond angles. In Fig. 10, a representative series of REDOR curves for IS_3, IS_2 and I_S spin systems, obtained by using the same bond lengths and angles, is shown which demonstrates the influence of the number of coupled spins. It is seen that the initial slope of the curve increases with the number of coupled nucleiwhich can be explained by the increase of the second moment M_2, due to heteronuclear dipolar coupling, in the same direction (see equation-2 for homonuclear coupling).

Table 1 summarizes the results from the fitting of the $^{11}B\{^{15}N\}$ REDOR curves in terms of heteronuclear dipolar coupling constants and the derived boron-nitrogen distances, the latter of which are also plotted in Fig. 11. All boron-nitrogen distances, obtained from the ^{11}B-^{15}N REDOR studies of the present precursor systems, are found to be longer than the value of 1.44Å derived from X-ray diffraction studies on pure *h*-BN [52]. The differences between the boron-nitrogen distances of precursor system-1 and 2 are negligible and are within the limits of error.

Finally, the scaling factors, obtained from the plateau values of the REDOR curves, are generally higher for precursor system-1 than for precursor system-2 which will be further commented below.

Table 1. *Derived boron-nitrogen distances and dipolar coupling constants d from analysis of the Experimental ^{11}B-^{15}N REDOR curves for Si-B-C-N ceramic samples from precursor polymers 1 and 2.*

Samples	Dipolar coupling constant, d [Hz]	Distance, rBN [A]	Scaling factor
1, 1960°C	1000	1.58 Å	0.85
1, 1800°C	1000	1.58 Å	0.95
1, 1700°C	1000	1.58 Å	0.95
1, 1600°C	1000	1.58 Å	0.95
1, 1500°C	1000	1.58 Å	0.95
1, 1400°C	1000	1.58 Å	0.95
1, 1050°C	930	1.61 Å	0.92
2, 1900°C	1050	1.55 Å	0.76
2, 1800°C	1050	1.55 Å	0.78
2, 1700°C	1050	1.55 Å	0.83
2, 1600°C	1050	1.55 Å	0.96
2, 1500°C	1050	1.55 Å	0.92
2, 1400°C	1050	1.55 Å	0.91
2, 1050°C	1050	1.55 Å	0.88
2, 800°C	1000	1.58 Å	0.80
2, 600°C	950	1.60 Å	0.80

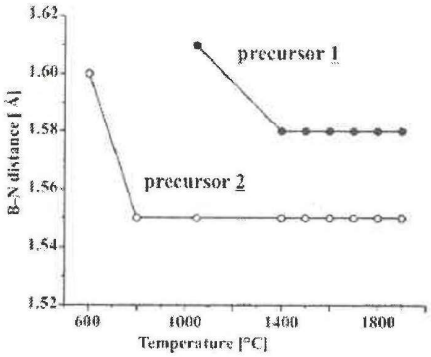

Figure 11.*Derived boron-nitrogen distances from analysis of the experimental 11B-15N REDOR curves for Si-B-C-N ceramic samples from precursor polymers 1 and 2.*

As mentioned earlier, for the theoretical REDOR curves, given in Figs. 8 and 9, either IS_3 (precursor system-1) or a superposition of IS_3, IS_2, IS and I spins systems (precursor system-2) were used with a single internuclear distance, although longer distances due to dipolar coupling with the nitrogen nuclei in the third coordination sphere or in different BN planes also might play a role (see Fig. 6). In Fig. 12 the influence of a second larger distance on the $^{11}B\{^{15}Ng\}$ REDOR curves is demonstrated by representative model calculations.

It is seen that a second distance has only a minor influence on the theoretical REDOR curves and is outside the accessible range, if in-plane distances compatible with the third coordination sphere of the boron atoms (distance a' in Fig. 6) are considered. The same holds for the ^{11}B-^{15}N heteronuclear dipolar interactions between the various BN planes (inter-plane distance c in Fig. 6). For this reason, a second, longer boron-nitrogen distance was not included in the present data analysis.

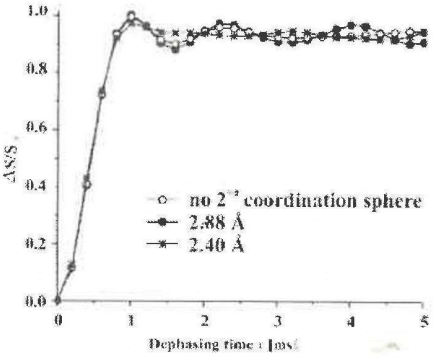

Figure 12. *Theoretical i1Bf15Ng REDOR curves obtained by considering a boron nucleus trigonally coordinated by three nitrogen nuclei at a distance of 1.55Å and three nitrogen nuclei in a second coordination sphere at the distances given in the figure (IS6 spin syste)]. For the relative position of the 15N nuclei the ideal h-BN Structure (See Figure 6) is assumed.*

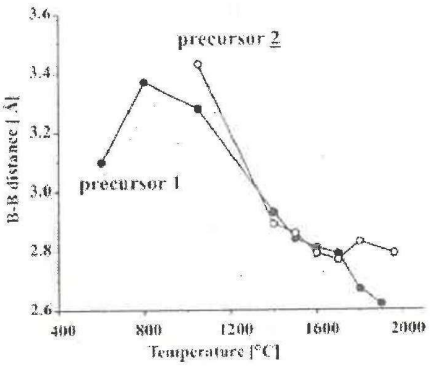

Figure 13. *Derived boron-boron distances from analysis of the experimental 11B spin echo decay curves for Si-B-C-N ceramic samples from precursor polymers 1 and 2.*

However, it is very likely that a better agreement between experiment and theory can be achieved by the consideration of a distribution of bond distances, as done earlier, for instance, in glasses [39]. Work along this line is in progress. Homonuclear boron-boron distances were obtained from analysis of ^{11}B spin echo decay curves for static samples (see experimental part). The derived distances are summarized in Table 2 and are plotted in Fig. 13. In general, very similar boron-boron distances are found for both precursor systems which steadily decrease from about 3.5 to 2.8Å in the temperature range between 800°C and 1900°C.

Table 2. *Derived boron-boron distances and second moments M_{2E} from analysis of the experimental ^{11}B spin echo decay curves for Si-B-C-N ceramic samples from precursor polymers 1 and 2.*

Samples	Dipolar coupling constant, d [Hz]	Distance, r_{BN} [Å]
1, 1960°C	5.9	2.79
1, 1800°C	5.4	2.83
1, 1700°C	6.1	2.77
1, 1600°C	5.9	2.79
1, 1500°C	5.0	2.86
1, 1400°C	4.7	2.89
1, 1050°C	1.7	3.43
2, 1900°C	8.6	2.62
2, 1800°C	7.7	2.67
2, 1700°C	5.8	2.79
2, 1600°C	5.6	2.81
2, 1500°C	5.3	2.84
2, 1400°C	4.4	2.93
2, 1050°C	2.2	3.28
2, 800°C	1.9	3.37
2, 600°C	5.1	3.10

Obviously, the temperature dependence for the boron-boron distance is much more pronounced than for the boron-nitrogen distance. Again, the derived boron-boron distances are larger than the value of 2.51 Å from X-ray studies on pure *h*-BN [53, 54]. However, they are consistent with the former $^{11}B\{^{15}N\}$ REDOR data and the resulting longer boron-nitrogen distances than in h-BN, as discussed above. For comparison, the same ^{11}B spin echo analysis was also done for pure h-BN. From this, a second moment of $8.8 \cdot 10^7$ rad^2/s^2 was obtained along with a boron-boron distance of 2.61Å , a value which is also 0.1Å larger than the aforementioned value from X-ray investigations. This deviation for the derived boron-boron distances from X-ray diffraction and ^{11}B spin echo analysis should be therefore kept in mind during the discussion of the internuclear distances for the ceramic systems of the present work.

In summary, the present $^{11}B\{^{15}N\}$ REDOR and ^{11}B spin echo experiments have provided the first quantitative data about the boronnitrogen and boron-boron distances in precursor-derived materials, covering a temperature range from about 800°C to 1900°C, including the amorphous-to-crystalline ceramic transformation. The derived results confirm the generally accepted model that the BNC_x phase consists of boron nitride sheets. The internuclear distances can be attributed to the in-plane distances in boron nitride (see Fig. 6), and thus prove a similar structure as in pure *h*-BN.

Both the boron-nitrogen and boron-boron distances, derived from the present NMR studies, are found to be somewhat larger than the values reported from X-ray diffraction studies on pure *h*-BN. However, it should be kept in mind that a somewhat longer boron-boron distance-2.61Å

instead of 2.51 Å from the X-ray study-was also found from the ^{11}B spin echo reference measurement on pure *h*-BN; the reason for this difference is not yet understood. Nevertheless, as can be seen from Table 2, except for the samples from precursor-2 heated at 1800°C and 1900°C, all derived boron-boron distances are distinct longer than the reference value from *h*-BN. The same is true for the boron-nitrogen distances derived from the $^{11}B\{^{15}N\}$ REDOR data, although in that case no reference measurements on a suitable model system were available.

Based on these results, it can be stated that the boron-boron and boron-nitrogen distances in the present precursor ceramics are consistently longer than those reported for pure *h*-BN. One explanation for this observation may be given by high-frequency bond librations resulting in smaller averaged dipolar interactions. Although such librational contributions cannot be ruled out completely, they would not explain the dependence on the thermal history. Hence, another discussed scenario is the presence of structural distortions in the BN layers. For instance, small nanodomains with sp^2-carbon sheets might be incorporated in the BN layers, which results in interdigitated structures along with bond distortions of the host layers. In this case, additional boron-carbon bonds are expected, for which a reliable experimental proof so far is missing. Likewise, separate but intercalated BN and sp^2-carbon (graphite-like) layers might be discussed, which do not require boron-carbon bond formation. Here again, the resulting internal stress would be partially compensated by bond distortions (i.e., increase of bond lengths) in the BN layers, in agreement with the findings from the present ^{11}B NMR studies.

The internuclear distances derived for both precursor systems are found to be quite similar. This also holds for the boron-nitrogen distances, shown in Fig. 11, where the observed small differences are within the limits of error. An interesting result is the almost identical temperature dependence for the boron-boron distance in both precursor systems (see Fig. 12), while for the boron-nitrogen distance a pronounced temperature dependence is absent. These findings indicate that structural rearrangements along with a better layer packing—as expressed by the shortening of the boron-boron distances—take place in the second coordination sphere, i.e., on a longer length-scale, even up to the highest pyrolysis temperature. At the same time, the local molecular structure (first coordinate sphere, boron-nitrogen distances) remains almost unaffected above 600°C.

A main difference between the present precursor systems can be seen for the REDOR plateaus, which is expressed by the scaling factors given in Table 1, and which indicate the average amount of bonded ^{15}N nuclei. Here, the samples from precursor system-2 with the higher carbon content exhibit lower plateau values than precursor system-1. This might indicate that for this particular system also sp2-carbon layers are incorporated in the BN layers which—as a direct consequence—give rise to a finite amount of boron-carbon bonds. However, it should be noted again that so far there is no evidence for boron-carbon bond formation in these systems. An independent proof or disproof could only be given by suitable ^{13}C double resonance NMR experiments which due to the very poor signalto-noise ratio of the ^{13}C NMR spectra for such systems at elevated pyrolysis temperatures are experimentally very demanding. Therefore, experiments on ^{13}C enriched samples should be performed along withmore experimental and theoretical work to provide a definitive picture for the structural composition of the BNC_x phase. Work along this line is in progress.

CONCLUSIONS

Precursor-derived Si-B-C-N ceramic systems were studied by solid-state NMR spectroscopy. The investigations presented here primarily address the structural composition of the BNC_x phase which plays a key role in the discussion of the high temperature stability of precursor-derived Si-B-C-N ceramics. Therefore, single and double resonance solid-state NMR experiments were employed which probe homonuclear and heteronuclear distances in two types of ^{15}N enriched precursor systems made from substituted polysilazenes and polysilylcarbodiimides. The results from $^{11}B\{^{15}N\}$REDOR and ^{11}B spin echo experiments proved the presence of layered structures as in *h*-BN. In general, the derived boron-nitrogen and boron-boron distances were almost identical in both precursor systems, but larger than in *h*-BN, which gives evidence for a distortion of the layers. In addition, the boron-boron distances, reflecting structural changes on a longer distance, were found to decrease with increasing pyrolysis temperature, while the short range order (expressed by the boron nitrogen distances) remains practically unaltered. On the

basis of the present results it is most likely that intercalated boron nitride and (amorphous) sp^2-carbon layers constitute the BNC_x phase. The graphite-like carbon layers create some internal pressure which in turn is responsible for the observed interatomic distance increase. However, further work is required to provide a comprehensive structural model for the BNC_x phase in such quaternary ceramic systems.

ACKNOWLEDGMENTS

Financial support for this research project by the Deutsche Forschungsgemeinschaft is gratefully acknowledged. O. Tsetsgee acknowledges financial support by the Deutsche Forschungsgemeinschaft and the Graduiertenkolleg No. 448 "Modern Methods of Magnetic Resonance in Materials Science."

REFERENCES

[1]. Lange, F.F. (1973) J. Am. Ceram. Soc., 56: 445.

[2]. Greil, P., Petzow, G., and Tanaka, H. (1987) Ceram. Int., 13: 19.

[3]. Lange, F.F. (1974) J. Am. Ceram. Soc., 57: 84.

[4]. Rice, R.W. (1983) Am. Ceram. Soc. Bull., 62: 916.

[5]. Seyferth, D. and Wiseman, G.H. (1984) J. Am. Ceram. Soc., 67: C-132.

[6]. Peuckert, M., Vaahs, T., and Brueck, M. (1990) Adv. Mater., 2: 398.

[7]. Bill, J. and Aldinger, F. (1995) Adv. Mater., 7: 775.

[8]. Baldus, H.P. and Jansen, M. (1997) Angew. Chem. Int. Ed. Engl., 36: 328.

[9]. Bill, J., Wakai, F., and Aldinger, F. (eds.) (1999) Grain Boundary Dynamics of Precursor-Derived Covalent Ceramics; Wiley-VCH: Weinheim.

[10]. Loeffelholz, J. and Jansen, M. (1995) Adv. Mater., 7: 289.

[11]. Weinmann, M., Schuhmacher, J., Kummer, H., Prinz, S., Peng, J., Seifert, H.J., Christ, M.,Mueller, K., Bill, J., and Aldinger, F. (2000) Chem. Mater., 12: 623.

[12]. Riedel, R., Kienzle, A., Dressler, W., Ruwisch, L., Bill, J., and Aldinger, F. (1996) Nature, 382: 796.

[13]. Schuhmacher, J., Berger, F., Weinmann, M., Bill, J., Aldinger, F., and Mueller, K. (2001) Appl.Organomet. Chem., 15: 809.

[14]. Jalowiecki, A., Bill, J., Aldinger, F., and Mayer, J. (1996) J. Composites, 27A: 717.

[15]. Bill, J., Kamphowe, T.W., Mueller, A., Wichmann, T., Zern, A., Weinmann, M., Schuhmacher, J., Mueller, K., Peng, J., Seifert, H.-J., and Aldinger, F. (2001) Appl. Organomet. Chem., 15: 1.

[16]. Bill, J., Schuhmacher, J., Mueller, K., Schempp, S., Seitz, J., Duerr, J., Lamparter, H.-P.,Golzcewski, J., Peng, J., Seifert, J., and Aldinger, F. (2000) Zeitschr. f. Metallk., 91: 335.

[17]. Spiess, H.W. (1985) Adv. Polym. Sci., 66: 23.

[18]. Eckert, H. (1992) Prog. NMR Spectrosc., 24: 59.

[19]. Schmidt-Rohr, K. and Spiess, H.W. (1994) Multidimensional Solid-State NMR and Polymers; Academic Press: London.

[20]. Fyfe, C.A. (1983) Solid-state NMR for Chemists; CFC Press: Guelph.

[21]. Lewis, R.H. and Maciel, G.E. (1995) J. Mater. Sci., 30: 5020.

[22]. Geradin, C.M., Taulelle, F., and Livage, J. (1993) Mater. Res. Soc. Symp. Proc., 287, 233.

[23]. Zhang, Z.F., Babonneau, F., Laine, R.M., Mu, Y., Harrod, J.F., and Rahn, J.A. J. (1991) Am. Ceram.Soc., 74: 670.

[24]. Laine, R.M., Babonneau, F., Rahn, J.A., Zhang, Z.F., and Youngdahl, K.A. (1991) 37th Sagamore Army Materials Research Conference Proceedings; Viechniki, D.J. (ed.); Publication Department of the Army.

[25]. Laine, R.M., Babonneau, F., Blowhowiak, K.Y., Kennish, R.A., Rahn, J.A., Exarhos, G.J., and Waldner, K.J. (1995) Am. Ceram. Soc., 78: 137.

[26]. Seitz, J., Bill, J., Egger, N., and Aldinger, F. (1996) J. Eur. Ceram. Soc., 16: 885.

[27]. Schuhmacher, J., Weinmann, M., Bill, J., Aldinger, F., and Mueller, K. (1998) Chem. Mater., 10: 3913.

[28]. Schmidt, W.R., Narsavage-Heald, D.M., Jones, D.M., Marchetti, P.S., Raker, D., and Maciel, G.E.(1999) Chem. Mater., 11: 1455.

[29]. Mueller, K. (1999) Grain Boundary Dynamics of Precursor-Derived Covalent Ceramics; Bill, J., Wakai, F.and Aldinger, F. (eds.); Wiley-VCH: Weinheim, 197.

[30]. Traßl, S., Suttor, D., Motz, G., Roessler, E., and Ziegler, G. (2000) J. Eur. Ceram. Soc., 20: 215.

[31]. Weinmann, M., Nast, S., Berger, F., Kaiser, G., Mueller, K., and Aldinger, F. (2001) Appl. Organomet.Chem., 15: 867.

[32]. Berger, F., Weinmann, M., Aldinger, F., and Mueller, K. (2004) Chem. Mater., 16: 919.
[33]. (33) Berger, F., Mueller, A., Aldinger, F., and Mueller, K.Z. (2005) Allg. Anorg. Chem., 631: 355.
[34]. Kumar, R., Prinz, S., Cai, Y., Zimmermann, A., Aldinger, F., Berger, F., and Mueller, K. (2005) Acta Materialia., 53: 4567.
[35]. Gullion, T. and Schaefer, J. (1989) Adv. Magn. Reson., 13: 57.
[36]. Gullion, T. and Schaefer, J. (1989) J. Magn. Reson., 81: 196.
[37]. Gullion, T. (1989) J. Magn. Reson., 85: 614.
[38]. Pan, Y., Gullion, T., and Schaefer, J. (1990) J. Magn. Reson., 90: 330.
[39]. Eckert, H., Elbers, S.A., Epping, J.D., Janssen, M., Kalwei, M., Strojek, W., and Voigt, U. (2004) Topics Curr. Chem., 246: 195.
[40]. Mueller, K.T. (1995) J. Magn. Reson., A 113: 81.
[41]. van Vleck, J.H. (1948) Phys. Rev., 33: 1168.
[42]. Gee, B. and Eckert, H. (1995) Solid State Nucl. Magn. Reson., 5: 113.
[43]. Haase, J. and Oldfield, E. (1993) J. Magn. Reson., A 101: 30.
[44]. Weinmann, M., Katz, S., Berger, F., Kaiser, G., Mueller, K., and Aldinger, F. (2001) Appl. Organomet.Chem., 15: 867.
[45]. Weinmann, M., Haug, R., Bill, J., Aldinger, F., Schuhmacher, J., and Mueller, K. (1997) J. Organomet. Chem., 541: 345.
[46]. Weinmann, M., Hoerz, M., Nast, S., Berger, F., Mueller, A., Kaiser, G., Mueller, K., and Aldinger, F.(2002) J. Organomet. Chem., 659: 29.
[47]. Bak, M., Rasmussen, J.T., and Nielsen, N.C. (2000) J. Magn. Reson., 147: 296.
[48]. Bak, M. and Nielsen, N.C. (1997) J. Magn. Reson., 125: 132.
[49]. Goetz, J.M. and Schaefer, J. (1997) J. Magn. Reson., 127: 147.
[50]. Schuhmacher, J., Mueller, K., Weinmann, M., Bill, J., and Aldinger, F. (1999) In Werkstoffwoche 98,Bd. VII; VCH: Weinheim, p. 321.
[51]. van Wuellen, L. and Jansen, M. (2005) Solid State Nucl. Magn. Reson., 27, 90.
[52]. Greenwood, N.N. and Earnshaw, A. (1988) Chemie der Elemente; VCH Berlin: Weinheim.
[53]. Pease, R.S. (1952) Acta Cryst., 5: 356.
[54]. Hagemayer, R.M., Mueller, U., Benmore, C.J., Neuefeind, J., and Jansen, M.J. (1999) Mater.Chem.; 9;2865